Research Square

Preprints are preliminary reports that have not undergone peer review.
They should not be considered conclusive, used to inform clinical practice,
or referenced by the media as validated information.

Development of CAR-T Therapy Targeting Two Distinct Epitopes of HER2 for Trastuzumab-Resistant Cancer

hyungseok Seo

h.seo@snu.ac.kr

Seoul National University https://orcid.org/0000-0002-6632-1208

Dong Hyun Kim

Seoul National University

Hyungwoo Jeong

Seoul National University

Sang-Eun Jung

Seoul National University

Seyon Kim

Seoul National University

Hayoung Kwon

Seoul National University

Hyung-Young Kim

Sungkyunkwan University

Chang Han Lee

Seoul National University College of Medicine https://orcid.org/0000-0002-7156-4423

Article

Keywords: HER2, CAR-T, Herceptin, nanobody, tandem CAR

Posted Date: November 3rd, 2026

DOI: https://doi.org/10.21203/rs.3.rs-11288684/v1

License: This work is licensed under a Creative Commons Attribution 4.0 International License.
Read Full License

Additional Declarations: There is no conflict of interest

Abstract

Alterations in the human epidermal growth factor receptor 2 (HER2) epitope recognized by trastuzumab-derived chimeric antigen receptors (CARs) may compromise tumor recognition. To diversify HER2 recognition, we generated CARs incorporating the camelid-derived H2H nanobody, the trastuzumab-derived 4D5 single-chain variable fragment, or both binders in two tandem orientations. We evaluated binding competition, murine and human CAR-T cell cytotoxicity, tumor growth, and tumor-infiltrating CAR-T cell phenotypes. H2H did not compete with 4D5 for HER2 binding, and H2H CAR-T cells retained cytotoxicity against targets expressing an engineered HER2 domain IV deletion variant that was poorly recognized by 4D5 CAR-T cells. In mice, H2H-4D5 suppressed the growth of wild-type HER2-expressing B16 tumors more effectively than the reverse tandem configuration, although survival did not differ significantly among groups. In a separate tumor-infiltrating lymphocyte analysis, H2H-4D5 CAR-T cells exhibited lower PD-1/TIM-3 co-expression and TOX expression than 4D5 CAR-T cells. All four human CAR configurations mediated cytotoxicity against breast cancer cells with endogenous HER2 expression. Human H2H-containing CAR-T cells, including both tandem configurations, also retained cytotoxicity against engineered mutant HER2-expressing tumor cells, whereas 4D5 CAR-T cells failed to eliminate these targets. These findings support complementary epitope recognition as a strategy to maintain HER2-directed CAR-T cell activity following disruption of the 4D5-binding region and identify binder orientation as a determinant of antitumor activity and exhaustion-associated phenotypes in the tested models.

Introduction

Chimeric antigen receptor (CAR) T cells are engineered T lymphocytes that express a synthetic receptor combining an extracellular antigen-binding domain with intracellular T-cell activation domains. Antigen recognition triggers intracellular signaling and T-cell activation, enabling CAR-T cells to specifically recognize and attack tumor cells[1,2]. The approval of Kymriah, the first CAR-T therapy for B-ALL, marked a new paradigm in cancer treatment. Although CAR-T therapy has produced remarkable clinical responses in hematologic malignancies, including lymphomas and leukemias, its efficacy in solid tumors remains limited[3]. Barriers to effective CAR-T therapy include toxicity, restricted trafficking, antigen heterogeneity, and a highly immunosuppressive tumor microenvironment that can promote CAR-T cell dysfunction and exhaustion[4,5].

Human epidermal growth factor receptor 2 (HER2), a member of the epidermal growth factor receptor (EGFR) family of receptor tyrosine kinases, regulates signaling pathways involved in proliferation, survival, and differentiation[6]. Aberrant HER2 expression has been identified in several cancers, notably breast, gastric, and ovarian cancers, making HER2 an important target for cancer immunotherapy[7,8]. Its clinical relevance is further supported by the association of HER2 expression with aggressive tumor growth, unfavorable prognosis, and increased metastatic potential[9]. These characteristics provide a rationale for HER2-targeted interventions. Trastuzumab, a monoclonal antibody that binds to domain IV

of the HER2 extracellular domain, has translated this rationale into an effective treatment for HER2-positive tumors. In patients with HER2-overexpressing breast or gastric cancer, trastuzumab has provided clinical benefits, including improved overall and progression-free survival, both as monotherapy and in combination with chemotherapy[10–12]. However, intrinsic and acquired resistance limit the durability of trastuzumab therapy and can lead to disease progression. Resistance may arise from heterogeneous HER2 expression or molecular alterations that reduce the abundance or accessibility of the targeted epitope[13,14]. In particular, loss of cell-surface HER2 following trastuzumab treatment and substitutions within the trastuzumab-binding interface, including P593R and V597M, have been associated with impaired trastuzumab activity[13,15]. These escape mechanisms may also compromise trastuzumab-derived HER2-targeted CAR-T cells, whose antigen-recognition domains retain the epitope specificity of the parental antibody. Although trastuzumab-derived HER2 CAR-T cells have demonstrated antitumor activity[16], reduced HER2 surface density or alterations in the shared binding interface may diminish CAR engagement and impair the elimination of resistant tumor cells. These limitations motivate alternative HER2-targeting approaches, particularly binders that recognize non-overlapping epitopes and may retain activity against trastuzumab-resistant HER2-positive tumors.

One strategy to overcome epitope-dependent tumor escape is to redesign the antigen-recognition domain of the CAR. Conventional CARs use single-chain variable fragments (scFvs) derived from monoclonal antibodies. For example, many HER2-directed CARs incorporate the trastuzumab-derived 4D5 scFv[17,18]. Nanobodies have emerged as compact alternatives to conventional antigen-binding domains. A nanobody comprises the variable domain of a camelid heavy-chain-only antibody (VHH) and mediates antigen recognition without an associated light chain[19]. Compared with scFvs, nanobodies offer potential advantages, including a smaller molecular size (approximately 15 kDa), favorable folding and stability, and access to recessed or sterically restricted epitopes[20,21]. These properties may be useful for targeting solid tumors, where antigen accessibility is an important consideration. Nanobody-based CARs may recognize HER2 epitopes that are inaccessible to conventional scFvs, broadening the targetable surface of HER2 and potentially preserving tumor recognition when the trastuzumab-binding site is altered. This provides a rationale for investigating nanobody-based CARs in solid tumors, where heterogeneous antigen expression and restricted epitope accessibility can compromise CAR-target engagement.

To address trastuzumab resistance and improve HER2-targeted CAR-T cell activity against solid tumors, we sought to diversify HER2 epitope recognition. We first generated a CAR incorporating H2H, a camelid-derived anti-HER2 nanobody that recognizes an epitope distinct from the trastuzumab/4D5-binding site. Because alterations in the trastuzumab-binding epitope can impair both antibody binding and recognition by 4D5-based CARs, the H2H CAR was designed to retain activity against HER2 variants associated with trastuzumab resistance. In parallel, we constructed tandem CARs containing the H2H nanobody and the trastuzumab-derived 4D5 scFv connected by a flexible (G4S)3 linker, enabling dual-epitope recognition of HER2. This design combines the distinct epitope specificity of H2H with the established HER2-targeting capacity of 4D5. We found that H2H and tandem CAR-T cells reduced tumor

growth *in vitro* and suppressed tumor progression *in vivo* in models expressing either wild-type HER2 or trastuzumab-resistant HER2 variants. In particular, H2H-4D5 tandem CAR-T cells exhibited significantly lower expression of exhaustion-associated markers. These findings support dual-epitope recognition as a strategy for maintaining antitumor activity when the trastuzumab-binding epitope is altered. The H2H-4D5 tandem CAR thus provides a framework for combining complementary antigen-binding domains to address epitope-specific resistance in HER2-directed CAR-T therapy.

Materials and methods

Cell preparation and ethics statement

The study protocols were approved by the institutional review board of Seoul National University and Samsung Medical Center (IRB No. E2512/004–005). All methods were performed in accordance with the approved guidelines. Leukapheresis was performed on whole blood from healthy donors at Samsung Medical Center to enrich peripheral blood mononuclear cells (PBMCs) according to standard protocols. Informed consent was obtained from each donor under the approved institutional review board protocol. Human T cells were isolated from PBMCs by negative selection using the EasySep™ Human T Cell Isolation Kit (STEMCELL, Vancouver, BC, Canada).

Mice

C57BL/6J mice (JA BIO Inc., Suwon, Korea) were used at 6–10 weeks of age after a one-week acclimation period. All procedures were approved by the Institutional Animal Care and Use Committee of Seoul National University (IACUC No. SNU-230104-1-4). The mice were anesthetized with 3% isoflurane and euthanized by CO_2 inhalation at a displacement rate of 30% of the chamber volume per minute.

CAR-T cell generation

For murine CAR-T cell generation, $CD8^+$ T cells were isolated from the spleens of C57BL/6 mice by negative selection using the EasySep™ Mouse $CD8^+$ T Cell Isolation Kit (STEMCELL). Purified $CD8^+$ T cells were activated for 24 h with 5 μg/mL plate-bound anti-CD3 and anti-CD28 antibodies (Bio X Cell, Lebanon, NH, USA). Following activation, cells were retrovirally transduced in the presence of 10 μg/mL polybrene and cultured in T-cell medium supplemented with 100 U/mL human IL-2. A second transduction was performed the following day using the same protocol, and the cells were cultured in medium containing 100 U/mL human IL-2 for an additional 3 days. For human CAR-T cell generation, purified T cells were cultured in RPMI 1640 medium supplemented with 10% fetal bovine serum, 0.1 mM HEPES, 1% nonessential amino acids (NEAA), and 1% L-glutamine. Cells were seeded and stimulated with Dynabeads Human T-Activator CD3/CD28 (Thermo Fisher Scientific, Waltham, MA, USA), then transduced with lentiviral vectors encoding anti-HER2 CARs 24 h after stimulation. Transduced cells

were cultured and expanded for 8 days in T-cell medium. Transduction efficiency was assessed by flow cytometry on days 7–9.

Viral vector design and production

The coding sequence of the HER2-specific scFv 4D5 was derived from the variable heavy- and light-chain regions of the humanized anti-HER2 antibody trastuzumab (huMAb4D5-8). A plasmid encoding the HER2 nanobody H2H was provided by Prof. Kisung Ko[22] from the Department of Medical Science, College of Medicine, Chung-Ang University. In the murine CAR constructs, the HER2-specific antigen-binding domain (4D5, H2H, 4D5-H2H, or H2H-4D5) was fused to murine CD28 and CD3ζ signaling domains. Thy1.1 served as a CAR detection marker and was linked to the CD28 signaling domain via a P2A sequence. In the human CAR constructs, the HER2-specific antigen-binding domain was fused to the human CD8α hinge and transmembrane domain, followed by 4-1BB and CD3ζ signaling domains. NGFR served as a CAR detection marker and was linked to the 4-1BB signaling domain via a T2A sequence. The open reading frames encoding the CAR constructs were subcloned into the pBABE retroviral expression vector or pELPs lentiviral expression plasmid using overlap-extension PCR.

The pBABE-puro-ERBB2 retroviral vector (Addgene plasmid #40978; Addgene, Watertown, MA, USA) was used as the parental construct for wild-type HER2 expression. To generate mutant HER2, 18 amino acids (Pro579–Cys596) were deleted from domain IV of pBABE-ERBB2 by inverse PCR. The entire plasmid, excluding the target region, was amplified using a pair of back-to-back primers. The PCR product was circularized using the NEBuilder HiFi DNA Assembly Kit (New England Biolabs, Ipswich, MA, USA).

Plat-E or Lenti-X™ 293T cells (Takara Bio Inc., Kusatsu, Japan) were used to produce viral vectors. Cells were seeded one day before transfection. Viral vectors were produced by co-transfecting the transfer plasmid with packaging plasmids (pMDLg/pRRE, pRSVrev, and pVSV-G for lentivirus; pCL-Eco for retrovirus) using Lipofectamine™ 2000 Transfection Reagent (Thermo Fisher Scientific). At 48–72 h after transfection, culture supernatants containing lentivirus were harvested and concentrated 20- to 50-fold using Lenti-X™ Concentrator reagent (Takara Bio). Concentrated virus was aliquoted and stored at − 80°C until use.

Cell lines

The human breast cancer cell lines SKBR3 and MDA-MB-468, the human B-cell precursor leukemia cell line Nalm-6, the murine melanoma cell line B16F0, and the murine T-cell lymphoma cell line EL4 were used in this study. SKBR3 and EL4 cells were purchased from the Korean Cell Line Bank (KCLB, Seoul, Korea). MDA-MB-468 cells were kindly provided by Prof. Chan Hyuk Kim. SKBR3, MDA-MB-468, and B16F0 cells were cultured in Dulbecco's modified Eagle medium (DMEM; Thermo Fisher Scientific) supplemented with 10% fetal bovine serum (FBS; Cytiva, Wilmington, DE, USA). Nalm-6 and EL4 cells were cultured in Roswell Park Memorial Institute (RPMI) 1640 medium (Thermo Fisher Scientific)

supplemented with 10% FBS (Cytiva). Cells were maintained in a humidified atmosphere containing 5% CO_2 at 37°C and routinely tested negative for mycoplasma. To generate HER2-expressing target cells, B16F0 and EL4 cells were transduced with a retrovirus encoding full-length human HER2 (ERBB2). Nalm-6 and MDA-MB-468 cells were co-transduced with lentiviruses encoding ffLuc-IRES-ZsGreen and HER2. Transduced cells were sorted using an SH800S Cell Sorter (Sony Biotechnology, San Jose, CA, USA).

In vivo studies

To establish tumors, 6- to 10-week-old C57BL/6J mice were injected subcutaneously with 0.3–1 × 10^6 B16F0-HER2 cells in 100 µL DPBS. On day 7, 5 × 10^6 CAR-T cells were adoptively transferred into tumor-bearing mice by retro-orbital injection. Tumor growth was monitored every 2–3 days using digital calipers, and tumor area (mm^2) was calculated as length × width. For TIL isolation, tumor-bearing mice received 5 Gy of irradiation on day 11 after tumor inoculation, followed by adoptive transfer of 5 × 10^6 CAR-T cells on day 12. On day 20, tumors were harvested and dissociated with collagenase D (1 mg/mL; Roche, Basel, Switzerland) and DNase I (100 µg/mL; Sigma-Aldrich, St. Louis, MO, USA) using a gentleMACS Dissociator (Miltenyi Biotec, Bergisch Gladbach, Germany).

Flow cytometric staining

Cells were stained for 30 min at 4°C with the following reagents: anti-mouse CD8 BV421, anti-rat CD90/mouse CD90.1 BV711, anti-mouse CD279 PE/Dazzle594, anti-mouse CD366 BV421, anti-human CD340 PE, anti-human CD271 APC, anti-human CD3 BV605, and anti-human CD8 PerCP/Cyanine5.5 (all from BioLegend, San Diego, CA, USA); Fixable Viability Dye eFluor780 (Invitrogen, Waltham, MA, USA); and anti-mouse CD62L APC-R700 and anti-mouse CD44 PE-Cy5 (both from BD Biosciences, San Jose, CA, USA). For intracellular staining, cells were incubated with Fix/Perm buffer (Thermo Fisher Scientific) for 30 min at 4°C after surface staining. Anti-human/mouse TCF1/TCF7 (C63D9) Alexa Fluor 647 (Cell Signaling, Danvers, MA, USA) and anti-human/mouse TOX PE (Invitrogen) antibodies were diluted 1:100 or 1:200 in permeabilization buffer (Invitrogen). Cells were resuspended in the antibody mixture and incubated for 1 h at 4°C.

In vitro cytotoxicity assay

Tumor cells were seeded into 96-well plates one day before real-time monitoring began. From day 0, mCherry or ZsGreen fluorescence intensity was monitored using the CELLCYTE X live-cell imaging system (CYTENA GmbH, Freiburg, Germany). CAR-T cells or untransduced T cells were added at different effector-to-target (E:T) ratios one or two days after monitoring began. For the rechallenge experiment, 100,000 tumor cells were added to each well, and monitoring continued for an additional 2 days.

ELISA

Plates were coated overnight at 4°C with 50 µL per well of 4D5 or H2H at 2 µg/mL. After blocking with 3% bovine serum albumin in PBS for 45 min, serial 10-fold dilutions of biotinylated HER2 (10 µM–10^{-5} µM) were added and incubated for 1 h at room temperature. The wells were washed three times with PBS containing 0.05% Tween 20 (PBST) and incubated with HRP-conjugated streptavidin (1:20,000; Abcam, Cambridge, UK; Cat# ab7403) for 1 h at room temperature. After three washes with PBST, signals were developed using 3,3',5,5'-tetramethylbenzidine (TMB) substrate (Thermo Fisher Scientific) and the reaction was stopped with 2 M H_2SO_4. Absorbance was measured at 450 nm using an Infinite 200 PRO NanoQuant microplate reader (Tecan, Männedorf, Switzerland).

Competitive ELISA

Plates were coated overnight at 4°C with 50 µL per well of 4D5 at 2 µg/mL and blocked with 3% skim milk in PBS. Biotinylated HER2 at a fixed concentration of 1 µM was mixed with H2H or 4D5 in a 1:5 molar ratio (HER2 to antibody) and preincubated for 2 h at room temperature. The mixtures were added to the plates and incubated for 1 h at room temperature. Bound biotinylated HER2 was detected using HRP-conjugated streptavidin and TMB substrate as described above. Absorbance was measured at 450 nm.

AlphaFold 3 modeling

HER2–anti-HER2 antibody complexes were predicted using the AlphaFold Server, based on AlphaFold 3[23]. The HER2 ECD and the heavy- or light-chain sequences of 4D5 or H2H were entered as separate protein entities, with one copy of each chain. For the tandem constructs, each antigen-binding domain (4D5-H2H or H2H-4D5), including the intervening $(G_4S)_3$ linker, was entered as a single continuous protein entity together with the HER2 ECD. The same prediction and ranking criteria were applied to all constructs. Predictions were generated using seeds 0–20, and the top-ranked model was used for analysis. Model confidence was evaluated using the ipTM score and interface PAE. The predicted HER2 structure was superposed onto HER2 chain C of the experimental HER2–Herceptin Fab structure (PDB ID: 1N8Z), and the Cα RMSD was calculated using PyMOL (version 3.1.6.1; Schrödinger, LLC, New York, NY, USA).

Statistical analysis

Statistical analyses were performed using GraphPad Prism v8.0 (GraphPad Software, San Diego, CA, USA). Data are presented as mean ± SEM. One-way ANOVA followed by Tukey's multiple-comparisons test was used to analyze cytotoxicity assays and tumor growth curves. One-way ANOVA followed by Dunnett's test was used for single-time-point tumor area comparisons. Survival curves were compared using the log-rank (Mantel–Cox) test.

Results

Design and functional analysis of 4D5 and H2H CAR-T cells

The human HER2-binding nanobody H2H was kindly provided by Prof. Kisung Ko[22]. We first predicted the binding sites of 4D5 and H2H on HER2 using AlphaFold 3 structural modeling. The models predicted that 4D5 binds to extracellular domain 4 (ECD 4), whereas H2H binds to ECD 3, suggesting distinct epitopes on HER2 (Fig. 1a). We then designed HER2-targeting H2H and 4D5 CAR constructs. Sequences encoding the H2H nanobody or 4D5 scFv were fused to sequences encoding the murine CD28 hinge, transmembrane, and costimulatory domains and the CD3ζ activation domain by PCR and subcloned into a retroviral expression vector. Thy1.1 was used as a CAR selection marker (Fig. 1b). Mouse CD8 + T cells were retrovirally transduced with the H2H or 4D5 CAR construct to generate the corresponding CAR-T cells. CAR expression was assessed by flow cytometry using the Thy1.1$^+$ selection marker (Fig. 1c). We next evaluated the cytotoxicity of murine 4D5 and H2H CAR-T cells by co-culturing them with HER2-overexpressing EL4-wtHER2-mCherry target cells (Fig. 1d). Both CAR-T cell products showed comparable cytotoxicity and antigen-specific killing of HER2-expressing targets (Fig. 1e). We then evaluated their *in vivo* antitumor activity in mice bearing HER2-overexpressing B16F0 tumors (Fig. 1f). H2H CAR-T cells delayed tumor growth compared with the DPBS control, whereas 4D5 CAR-T cells showed greater antitumor efficacy (Fig. 1g and 1h). No significant differences in survival were observed among the groups (Fig. 1i). These results demonstrate antigen-specific cytotoxicity in vitro and antitumor activity in vivo for both H2H and 4D5 CAR-T cells.

H2H and 4D5 CAR-T cells recognize distinct HER2 epitopes

To determine whether H2H and 4D5 engage distinct HER2 epitopes, we performed a cross-competition ELISA (Fig. 2a). Biotinylated recombinant HER2 was preincubated for 1 h with PBS (negative control, N.C.), H2H, or 4D5 before being added to plate-bound 4D5 IgG. Captured HER2 was detected using streptavidin-HRP (Fig. 2b). Preincubation with H2H produced a signal comparable to that of the negative control, whereas preincubation with 4D5 scFv abolished capture, indicating that H2H does not occlude the 4D5 epitope. We next compared the apparent HER2-binding affinities of H2H and 4D5 (Fig. 2c). Under these assay conditions, 4D5 showed a higher apparent binding affinity than H2H.

To determine whether an H2H-based CAR could overcome resistance caused by loss of trastuzumab-binding residues, we generated a mutant HER2 (mtHER2) protein lacking key residues within the 4D5-binding interface in ECD 4 (Fig. 2d). EL4 cell lines stably expressing wild-type HER2 (wtHER2) or mtHER2 were established by retroviral transduction. Surface HER2 staining was modestly lower in EL4-mtHER2 cells than in EL4-wtHER2 cells (Fig. 2e and 2f). H2H or 4D5 CAR-T cells were then co-cultured with EL4-mtHER2-mCherry target cells (Fig. 2g). The cytotoxicity of 4D5 CAR-T cells against mtHER2 targets was no greater than that of untransduced (UTD) T cells. In contrast, H2H CAR-T cells showed significantly greater cytotoxicity against these targets (Fig. 2h). Together, these findings suggest that H2H recognizes

a HER2 epitope distinct from that of 4D5 and retains cytolytic activity against a HER2 variant with a disrupted 4D5 epitope.

Design and functional analysis of 4D5-H2H and H2H-4D5 tandem CAR-T cells

Tandem CARs incorporate two distinct antigen-binding domains within a single receptor and have been reported to broaden target coverage, improve efficacy and safety, and reduce relapse rates[24]. We hypothesized that simultaneous engagement of two non-overlapping HER2 epitopes would increase functional avidity while limiting mutation-driven antigenic escape. We therefore designed tandem CARs containing both antigen-binding domains in opposite N-to-C-terminal orientations, designated 4D5-H2H and H2H-4D5 (Fig. 3a and 3b). We first modeled the CAR-HER2 complexes *in silico* using AlphaFold 3 (Supplemental Fig. 1a and 1b). H2H alone was predicted to engage ECD 3 of HER2, consistent with its lack of competition with 4D5 for binding (Fig. 1a). In the tandem configurations, the H2H moiety was predicted to contact ECD 3 and ECD 2 respectably, whereas the predicted 4D5 binding mode remained essentially unchanged across models. One possible interpretation is that the higher-affinity 4D5 moiety dominates the predicted interface, while the lower-affinity H2H moiety adopts a geometry permitted by the linker (Fig. 2c).

We next generated four HER2-targeting CAR-T cell products, 4D5, H2H, 4D5-H2H, and H2H-4D5 (Fig. 3c), and compared their cytotoxicity against EL4-wtHER2-mCherry target cells using live-cell imaging. To assess the durability of effector function, cultures were rechallenged with 1×10^5 tumor cells on day 4 (Fig. 3d). The result showed that all three H2H-containing constructs produced a more rapid and sustained decrease in mCherry signal than 4D5 CAR-T cells at every effector-to-target (E:T) ratio (Fig. 3e–g). Next, to evaluate *in vivo* antitumor activity of these CAR-T cells, UTD T cells or the corresponding murine 4D5, H2H, 4D5-H2H, or H2H-4D5 CAR-T cells were adoptively transferred into mice bearing B16F0-HER2 tumors (Fig. 3h). The result demonstrated that treatment with 4D5 or H2H-4D5 CAR-T cells led to a substantial inhibition of tumor growth and an enhancement of survival outcomes when compared to remaining group. (Fig. 3i-j and Supplementary Fig. 2). These data identify H2H-4D5 as a tandem configuration that retains the *in vivo* activity of 4D5 while incorporating recognition of a second, non-overlapping HER2 epitope.

Phenotypic and functional characterization of tumor-infiltrating HER2 tandem CAR-T cells

Given the differences in HER2 binding strength between the HER2 binding domain of CARs (Fig. 2c), we examined the differentiation and exhaustion-associated phenotypes of CAR-T cells within tumors. UTD T cells or 4D5, H2H, 4D5-H2H, or H2H-4D5 CAR-T cells were adoptively transferred into C57BL/6 mice bearing B16F0-HER2 tumors on day 12 after tumor inoculation. Tumor-infiltrating lymphocytes (TILs) were isolated on day 20, and CAR^+ cells were analyzed by flow cytometry (Fig. 4a). Tumor size was comparable among all CAR-T cell treatment groups on day 17 after tumor inoculation (Fig. 4b). CAR^+ TILs predominantly exhibited an effector-memory ($CD44^+CD62L^-$) phenotype across groups, consistent

with sustained antigen exposure within tumors. However, the central-memory ($CD44^+CD62L^+$) fraction was approximately twofold higher in recipients of H2H CAR-T cells than in recipients of 4D5, 4D5-H2H, or H2H-4D5 CAR-T cells (Fig. 4c), suggesting less terminal differentiation in constructs with H2H in the membrane-distal position.

We next assessed exhaustion-associated markers. PD-1 and TIM-3 co-expression was high in 4D5, H2H, and 4D5-H2H CAR^+ TILs but was significantly lower in H2H-4D5 CAR^+ TILs (Fig. 4d). Intracellular staining for TCF-1 and TOX, transcription factors associated with memory formation and exhaustion, respectively, also showed significantly lower TOX expression in H2H-4D5 TILs (Fig. 4e). These findings suggest reduced engagement of a TOX-associated exhaustion program in tumor-infiltrating H2H-4D5 CAR-T cells. The $TCF\text{-}1^-TOX^-$ subset was correspondingly expanded in H2H-4D5 TILs. To examine the activation and proliferative status of this compartment, we assessed PD-1 and Ki67 expression. $PD\text{-}1^+Ki67^+$ cells were most frequent in H2H-4D5 TILs and were significantly more frequent than in 4D5-H2H TILs (Fig. 4f), consistent with an antigen-experienced, actively cycling phenotype within the $TCF\text{-}1^-TOX^-$ compartment.

Together, the TIL analyses showed that H2H-4D5 tandem CAR-T cells exhibited a less pronounced exhaustion-associated phenotype than 4D5 CAR-T cells. These findings suggest that positioning the lower-affinity H2H moiety in the membrane-distal, antigen-proximal position may modulate HER2 engagement to support antitumor activity while limiting signals that drive terminal exhaustion.

Design and in vitro comparison of human CAR-T cells

To determine whether the properties of the four anti-HER2 CAR configurations were retained in human CAR-T cells, we constructed corresponding human CARs using the same antigen-binding domains as the murine constructs. Each receptor comprised a 4D5, H2H, 4D5-H2H, or H2H-4D5 antigen-binding domain fused to a human CD8α hinge and transmembrane region, a 4-1BB costimulatory domain, and a CD3ζ signaling domain, followed by a T2A-linked LNGFR selection marker (Fig. 5a). Peripheral blood T cells from a healthy donor were transduced with lentiviral vectors, and CAR expression was assessed using LNGFR staining (Fig. 5b). We next compared cytotoxicity against SKBR3-fluc-mCherry cells, a HER2-amplified human breast adenocarcinoma line that expresses HER2 from its endogenous locus. Tumor cells were seeded, and CAR-T cells were added on day 2 at E:T ratios ranging from 1:1 to 4:1. Tumor burden was monitored by live-cell imaging of total mCherry fluorescence intensity (Fig. 5c). All four CAR-T cell products reduced the mCherry signal at every E:T ratio (Fig. 5d–f), consistent with the murine CAR-T cell results (Fig. 3). To determine whether H2H or tandem CAR-T cells could eliminate trastuzumab-resistant target cells, we co-cultured the four CAR-T cell products with human Nalm-6 cells (Fig. 5g and 5h) or MDA-MB-468 breast cancer cells (Fig. 5i and 5j) expressing wtHER2 or mtHER2. H2H, 4D5-H2H, and H2H-4D5 CAR-T cells effectively killed both wtHER2- and mtHER2-expressing target cells, whereas 4D5 CAR-T cells failed to eliminate mtHER2-expressing target cells. The findings indicate that H2H-containing CAR-T cells, notably H2H-4D5 tandem CAR cells, exhibit functionality against trastuzumab-resistant tumor cells that present alterations in the HER2 binding epitope.

Discussion

Despite the promising potential of trastuzumab as an effective antibody therapy against HER2-expressing tumor including breast and gastric cancer, the development of resistance to trastuzumab by cancer cells poses significant challenges to antibody-based immunotherapy and CAR-T therapy. Complementary epitope recognition may broaden the activity of HER2-directed CAR-T cells against variants that compromise recognition by individual binders. In this study, H2H-containing CAR-T cells retained cytotoxicity against engineered mtHER2 targets that were poorly recognized by trastuzumab based 4D5 CAR-T cells. Combining H2H and 4D5 in tandem receptors also revealed orientation-dependent differences in antitumor activity and tumor-infiltrating T-cell phenotypes. H2H-4D5 showed activity against mtHER2 in vitro, suppressed tumor growth in a wild-type HER2-expressing model, and exhibited lower expression of selected exhaustion-associated markers in a separate TIL analysis. These findings support further evaluation of epitope complementarity and receptor architecture in HER2-directed CAR design.

Antigen escape through alteration of a targeted determinant, rather than loss of the antigen itself, is a recurring mechanism of resistance to receptor-based immunotherapy. In B-cell acute lymphoblastic leukemia, CD19-negative relapse following CD19 CAR-T therapy can arise not only from transcriptional silencing but also from alternative splicing, acquired mutations, epitope masking, and trogocytosis, each of which preserves the antigen while rendering the targeted epitope inaccessible[25]. Similarly, in patients with HER2-expressing breast cancer, Chen et al. identified HER2 downregulation and the trastuzumab-interface substitutions P593R and V597M as mechanisms associated with resistance to trastuzumab deruxtecan (T-DXd)[13,15]. Because 4D5-derived CARs inherit the epitope specificity of the parental antibody, these alterations may also compromise HER2 CAR engagement. Our approach diversifies recognition within a single antigen. Nanobody-based tandem CAR studies indicate that combining binding domains does not invariably produce additive activity[26]. The value of H2H-4D5 therefore lies in its dual recognition of HER2 and its observed functional activity. Whether cooperative binding contributes to this activity remains to be determined. A single-receptor format may also help ensure that each successfully modified T cell carries both recognition domains, although balanced surface display and binding activity require direct confirmation.

Previous studies of soluble anti-HER2 VHH-Fc antibodies support the potential of alternative binders in trastuzumab-resistant models, albeit in a different therapeutic format[22]. Our approach focuses on recognizing different epitopes within a single antigen rather than expanding the number of target antigens. The tandem design addresses the distinct strengths of the individual binders. H2H supported mutant recognition, whereas 4D5 showed greater tumor suppression in the initial *in vivo* comparison (Figs. 1 and 2). H2H-4D5 tandem CAR combined these properties within a single receptor, although 4D5-H2H CAR neither superiority over 4D5 nor a survival advantage was established (Fig. 3).

The differences between reciprocal tandem configurations suggest that domain order influences productive CAR engagement. Extracellular spacer design and binder properties can affect tumor recognition, and affinity tuning can alter the antigen-density requirements of HER2 CAR-T cells[27,28]. We

hypothesize that positioning H2H distally changes epitope accessibility or the duration and organization of receptor engagement. Altered engagement geometry may permit effective target killing while limiting prolonged stimulation, but this hypothesis should be tested alongside possible differences in receptor expression and antigen exposure. The ELISA measurements describe apparent binding under the assay conditions and do not establish the affinity or functional avidity of membrane-bound tandem receptors (Fig. 2a and 2b). Similarly, the variable H2H contact regions predicted across structural models represent candidate configurations that require validation. Noncompetition with 4D5 supports compatible recognition under the conditions tested but does not resolve the H2H epitope or demonstrate simultaneous engagement by both domains. Direct binding and signaling measurements are needed to connect receptor geometry with the observed functional differences.

An unexpected observation was that two tandem CARs differing only in the order of the same two binding domains showed differences in both antitumor activity and TIL differentiation (Figs. 3 and 4). H2H-4D5 CAR TILs exhibited lower PD-1/TIM-3 co-expression and TOX expression, suggesting an altered response to stimulation within the tumor (Fig. 4). This observation is consistent with evidence that receptor signaling can shape CAR-T cell exhaustion[29] and that TOX-family transcription factors participate in exhaustion-associated regulatory networks[30]. Because TOX contributes to the epigenetic program of exhaustion and its antagonism can redirect exhausted $CD8^+$ T cells toward durable effector-like states[31], reduced TOX expression in H2H-4D5 TILs may reflect engagement that limits commitment to terminal exhaustion. Nevertheless, the expanded $TCF\text{-}1^-TOX^-$ population in H2H-4D5 TILs requires careful interpretation (Fig. 4e). Although the enrichment of $PD\text{-}1^+Ki67^+$ cells indicates a cycling compartment without directly establishing cytotoxic competence or long-term persistence, the less exhausted phenotype of H2H-4D5 CAR-T cells was accompanied by improved tumor control and prolonged survival. Together, these observations suggest an association between reduced exhaustion and enhanced antitumor efficacy but do not establish a causal relationship.

The activity of the corresponding human CAR-T cells provides an additional basis for translational investigation. Recognition of SK-BR-3 cells demonstrates activity against endogenous HER2, while the elimination of engineered trastuzumab resistant mtHER2 targets supports the preservation of complementary recognition in human T cells (Fig. 5). H2H containing human CAR-T cells significantly control both wtHER2 or mtHER2 expressing tumor cells, while the 4D5 single CAR-T cell does not appear to eliminate mtHER2-expressing cells. Further evaluation is required to ascertain the efficacy of the model in patient-derived resistant models and to determine the size of the therapeutic window. A serious adverse event following ERBB2 CAR-T cell administration demonstrated the potential risks of this target[32], while subsequent HER2 CAR studies have reported clinical activity alongside dose-related toxicities[33]. Broader epitope recognition may enhance tumor coverage but does not intrinsically improve discrimination between malignant cells and normal tissues expressing HER2. Reducing affinity may favor discrimination against normal targets with low antigen density but could also compromise recognition of heterogeneous tumors. Our approach of incorporating a second binding domain through

the application of nanobody-based tandem CAR has the considerable potential to further shape the balance.

This study identifies H2H as a complementary HER2-binding domain that enables CAR-T cell activity against an engineered HER2 variant with a disrupted 4D5 epitope. Among the tandem configurations, H2H-4D5 retained the in vivo antitumor activity of 4D5 and exhibited a less pronounced exhaustion-associated phenotype in tumor-infiltrating CAR-T cells. Human H2H-containing CAR-T cells also retained cytotoxicity against both wild-type and mutant HER2-expressing targets, supporting the functional relevance of complementary recognition across the tested platforms. Although engineered models and differences between efficacy and TIL study conditions limit mechanistic interpretation, these results provide a basis for further evaluation. The primary research objectives are to test clinically observed HER2 variants at matched antigen densities and to examine receptor engagement and signaling, functional persistence, and normal-tissue reactivity. Together, these findings support further development of H2H-4D5 and highlight complementary epitope recognition and binding-domain orientation as important considerations in HER2 CAR design.

Abbreviations

HER2 Receptor tyrosine-protein kinase erbB-2

CAR-T Chimeric Antigen Receptor-T

scFv single-chain variable fragment

CM central memory

EM effector memory

wt wild-type

mt mutant

Declarations

Conflicts of interest

The authors declare no conflicts of interest.

Author contributions

All authors contributed to writing the manuscript. D.H.K., H.W.J., S.E.J., S.K., and H.Y.K. performed the experiments. D.H.K., H.W.J., and S.K. created the figures. H.S. oversaw the project and provided overall

guidance.

Acknowledgments

H.S. received funding from the Creative-Pioneering Researchers Program at Seoul National University. This work was also supported by National Research Foundation of Korea (NRF) through grants RS-2023-00242443, RS-2023-00210035, RS-2024-00406325, and RS-2024-00451880; Korea Drug Development Fund (KDDF) (RS-2023-00282907), funded by the Korean government (MSIT); and Korea Institute for Advancement of Technology (KIAT) grant funded by the Korean government (MOTIE) (RS-2025-02214034, HRD Program for Industrial Innovation).

Data availability statement

The data supporting the findings of this study are available from the corresponding author upon reasonable request.

Sources of support

H.S. received funding from the Creative-Pioneering Researchers Program at Seoul National University. This work was also supported by National Research Foundation of Korea (NRF) through grants RS-2023-00242443, RS-2023-00210035, RS-2024-00406325, and RS-2024-00451880; Korea Drug Development Fund (KDDF) (RS-2023-00282907), funded by the Korean government (MSIT); and Korea Institute for Advancement of Technology (KIAT) grant funded by the Korean government (MOTIE) (RS-2025-02214034, HRD Program for Industrial Innovation).

References

1. June, C. H., O'Connor, R. S., Kawalekar, O. U., Ghassemi, S. & Milone, M. C. CAR T cell immunotherapy for human cancer. *Science* 359, 1361–1365 (2018).
2. Sadelain, M., Brentjens, R. & Rivière, I. The basic principles of chimeric antigen receptor design. *Cancer discovery* 3, 388–398 (2013).
3. Maude, S. L. *et al.* Chimeric antigen receptor T cells for sustained remissions in leukemia. *New England Journal of Medicine* 371, 1507–1517 (2014).
4. Sterner, R. C. & Sterner, R. M. CAR-T cell therapy: current limitations and potential strategies. *Blood cancer journal* 11, 69 (2021).
5. Kim, J. *et al.* Strategies to Overcome Hurdles in Cancer Immunotherapy. *Biomaterials Research* 28, 0080 (2024).
6. Rubin, I. & Yarden, Y. The basic biology of HER2. *Annals of oncology* 12, S3–S8 (2001).

7. Yan, M. *et al.* HER2 expression status in diverse cancers: review of results from 37,992 patients. *Cancer and Metastasis Reviews* 34, 157–164 (2015).
8. Yarden, Y. & Sliwkowski, M. X. Untangling the ErbB signalling network. *Nature reviews Molecular cell biology* 2, 127–137 (2001).
9. Cheng, X. A comprehensive review of HER2 in cancer biology and therapeutics. *Genes* 15, 903 (2024).
10. Slamon, D. J. *et al.* Use of chemotherapy plus a monoclonal antibody against HER2 for metastatic breast cancer that overexpresses HER2. *New England journal of medicine* 344, 783–792 (2001).
11. Bang, Y.-J. *et al.* Trastuzumab in combination with chemotherapy versus chemotherapy alone for treatment of HER2-positive advanced gastric or gastro-oesophageal junction cancer (ToGA): a phase 3, open-label, randomised controlled trial. *The Lancet* 376, 687–697 (2010).
12. Hudis, C. A. Trastuzumab—mechanism of action and use in clinical practice. *New England journal of medicine* 357, 39–51 (2007).
13. Chen, W. *et al.* Trastuzumab Deruxtecan Resistance via Loss of HER2 Expression and Binding. *Cancer Discov* 16, 235–249 (2026).
14. Mosele, F. *et al.* Trastuzumab deruxtecan in metastatic breast cancer with variable HER2 expression: the phase 2 DAISY trial. *Nat Med* 29, 2110–2120 (2023).
15. Kong, X. *et al.* Mechanism of trastuzumab resistance caused by HER-2 mutation in breast carcinomas. *Cancer management and research*, 5971–5982 (2019).
16. Zhao, Y. *et al.* A herceptin-based chimeric antigen receptor with modified signaling domains leads to enhanced survival of transduced T lymphocytes and antitumor activity. *The Journal of Immunology* 183, 5563–5574 (2009).
17. Tóth, G., Szöllősi, J., Abken, H., Vereb, G. & Szöőr, Á. A small number of HER2 redirected CAR T cells significantly improves immune response of adoptively transferred mouse lymphocytes against human breast cancer xenografts. *International Journal of Molecular Sciences* 21, 1039 (2020).
18. Hegde, M. *et al.* Tumor response and endogenous immune reactivity after administration of HER2 CAR T cells in a child with metastatic rhabdomyosarcoma. *Nature communications* 11, 3549 (2020).
19. Muyldermans, S. *et al.* Camelid immunoglobulins and nanobody technology. *Veterinary immunology and immunopathology* 128, 178–183 (2009).
20. Muyldermans, S. Nanobodies: natural single-domain antibodies. *Annual review of biochemistry* 82, 775–797 (2013).
21. Bannas, P., Hambach, J. & Koch-Nolte, F. Nanobodies and nanobody-based human heavy chain antibodies as antitumor therapeutics. *Frontiers in immunology* 8, 1603 (2017).
22. Park, C. *et al.* Plant-Derived Anti-Human Epidermal Growth Factor Receptor 2 Antibody Suppresses Trastuzumab-Resistant Breast Cancer with Enhanced Nanoscale Binding. *ACS Nano* 18, 16126–16140 (2024).

23. Abramson, J. *et al.* Addendum: Accurate structure prediction of biomolecular interactions with AlphaFold 3. *Nature* 636, E4 (2024).
24. Gomez-Melero, S. *et al.* Tandem CAR-T cell therapy: recent advances and current challenges. *Front Immunol* 16, 1546172 (2025).
25. Aparicio-Perez, C., Carmona, M., Benabdellah, K. & Herrera, C. Failure of ALL recognition by CAR T cells: a review of CD 19-negative relapses after anti-CD 19 CAR-T treatment in B-ALL. *Front Immunol* 14, 1165870 (2023).
26. De Munter, S. *et al.* Nanobody Based Dual Specific CARs. *Int J Mol Sci* 19 (2018).
27. Hudecek, M. *et al.* Receptor affinity and extracellular domain modifications affect tumor recognition by ROR1-specific chimeric antigen receptor T cells. *Clin Cancer Res* 19, 3153–3164 (2013).
28. Liu, X. *et al.* Affinity-Tuned ErbB2 or EGFR Chimeric Antigen Receptor T Cells Exhibit an Increased Therapeutic Index against Tumors in Mice. *Cancer Res* 75, 3596–3607 (2015).
29. Ahn, T., Bae, E. A. & Seo, H. Decoding and overcoming T cell exhaustion: Epigenetic and transcriptional dynamics in CAR-T cells against solid tumors. *Mol Ther* 32, 1617–1627 (2024).
30. Seo, H. *et al.* TOX and TOX2 transcription factors cooperate with NR4A transcription factors to impose CD8(+) T cell exhaustion. *Proc Natl Acad Sci U S A* 116, 12410–12415 (2019).
31. Beltra, J. C. *et al.* Stat5 opposes the transcription factor Tox and rewires exhausted CD8(+) T cells toward durable effector-like states during chronic antigen exposure. *Immunity* 56, 2699–2718 e2611 (2023).
32. Morgan, R. A. *et al.* Case report of a serious adverse event following the administration of T cells transduced with a chimeric antigen receptor recognizing ERBB2. *Mol Ther* 18, 843–851 (2010).
33. Hegde, M. *et al.* Autologous HER2-specific CAR T cells after lymphodepletion for advanced sarcoma: a phase 1 trial. *Nat Cancer* 5, 880–894 (2024).

Figures

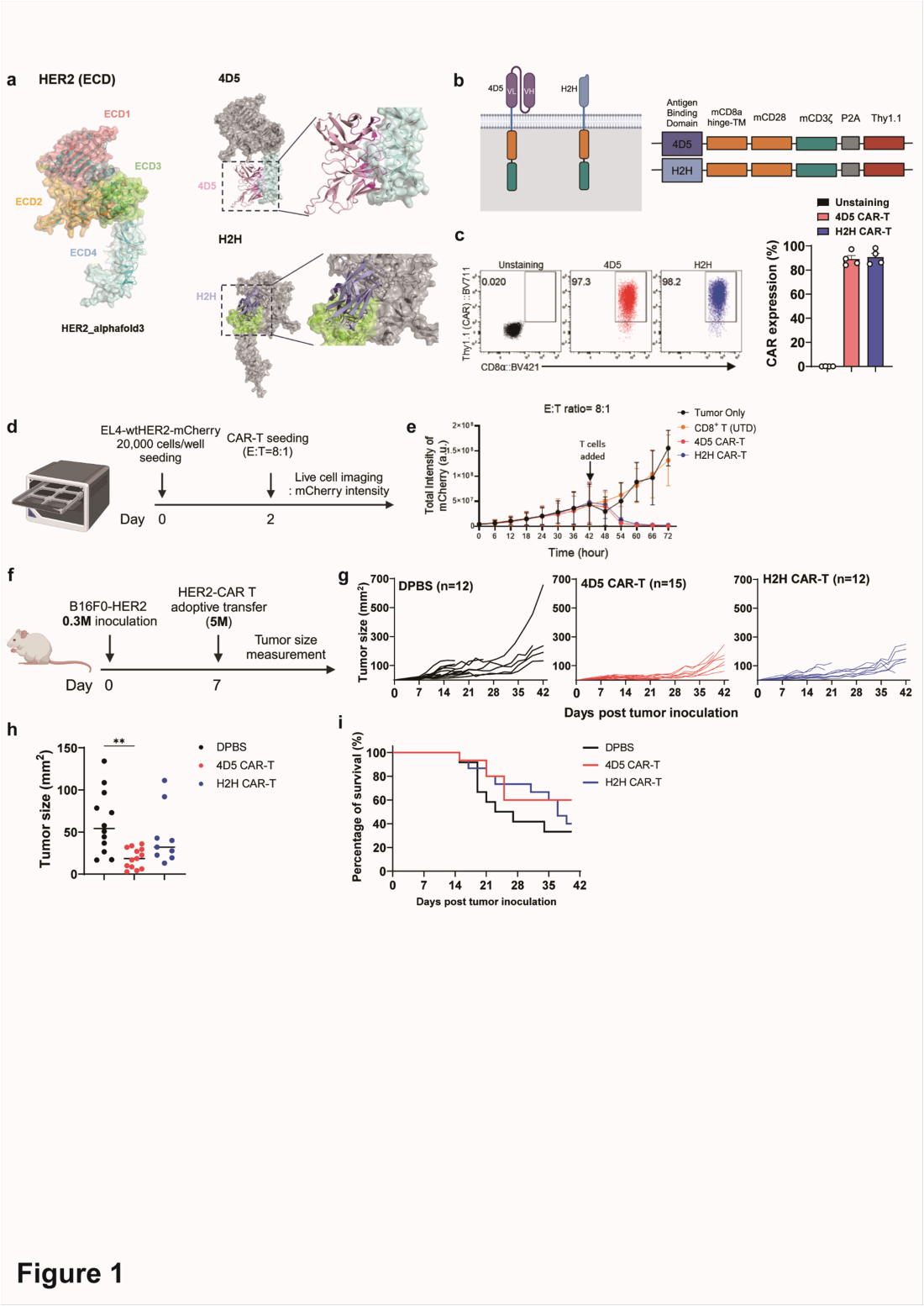


Figure 1

Figure 1

Structural and functional characterization of HER2-targeting 4D5 and H2H CAR-T cells.

(a) Structural models of the HER2 extracellular domain (ECD) with the predicted binding interfaces of 4D5 and H2H, highlighting distinct epitope recognition patterns. (b) Schematic of the 4D5 and H2H CAR constructs, showing the antigen-binding domains and intracellular signaling components. (c)

Representative flow cytometry plots and quantification of CAR expression in transduced T cells. (d) Experimental design of the cytotoxicity assay using EL4-HER2-mCherry target cells and CAR-T cells at an effector-to-target (E:T) ratio of 8:1. (e) Time-course analysis of HER2 CAR-T cell-mediated cytotoxicity, measured by total mCherry fluorescence intensity. (f) Experimental design for the evaluation of in vivo antitumor activity. (g–i) Tumor growth and survival following treatment with DPBS, 4D5 CAR-T cells, or H2H CAR-T cells: (g) tumor growth curves, (h) tumor size on day 17 after inoculation, and (i) survival curves. Data are presented as mean ± SEM. Statistical significance was determined by one-way ANOVA (*P < 0.05, **P < 0.01, ***P < 0.001, ****P < 0.0001).

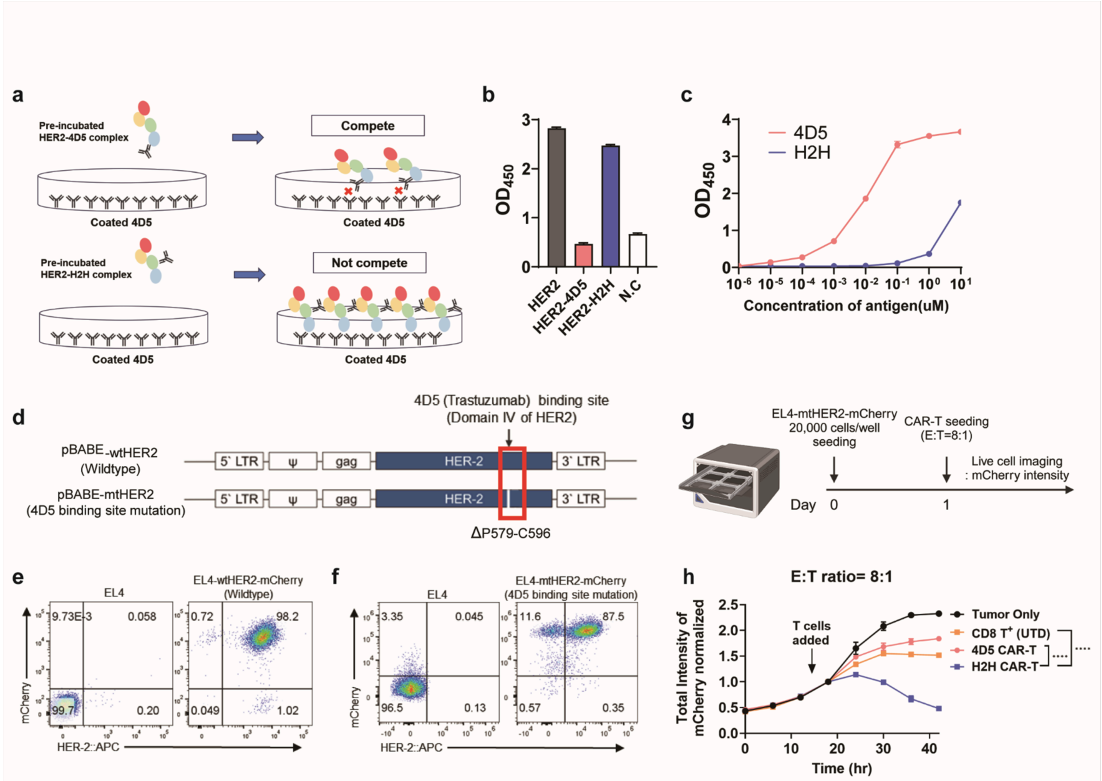


Figure 2

Figure 2

Binding properties of H2H and 4D5 and CAR-T cell cytotoxicity against targets with an altered 4D5-binding site.

(a) Schematic of the competition assay used to evaluate H2H and 4D5 binding to HER2. (b) Quantification of binding competition using HER2 alone (HER2), HER2 preincubated with 4D5 (HER2-

4D5), or HER2 preincubated with H2H (HER2-H2H). (c) Apparent binding curves for 4D5 and H2H across a range of antigen concentrations. (d) Schematic of the HER2 constructs, including mutant HER2 (mtHER2) with an altered 4D5-binding site. (e-f) Flow cytometric analysis of HER2 and mCherry expression in EL4 cells transduced with wtHER2 (e) or mtHER2 (f). (g) Experimental design of the cytotoxicity assay using EL4-mtHER2-mCherry target cells and CAR-T cells at an effector-to-target (E:T) ratio of 8:1. (h) Cytotoxicity of 4D5 and H2H CAR-T cells against tumor cells with an altered 4D5-binding site. Data are presented as mean ± SEM. Statistical significance was determined by one-way ANOVA (*P < 0.05, **P < 0.01, ***P < 0.001, ****P < 0.0001).

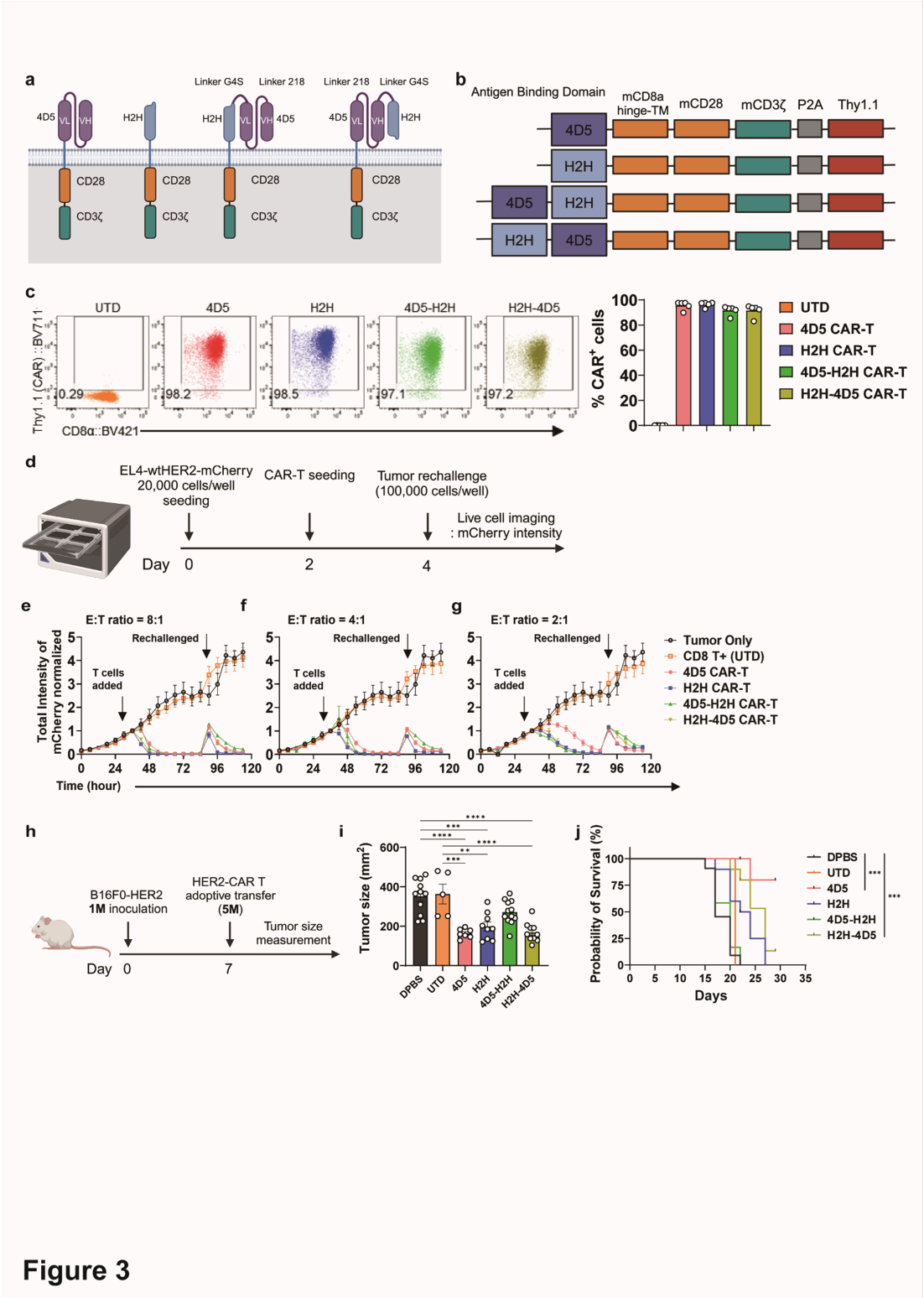


Figure 3

Figure 3

Design, structural modeling, and in vitro and in vivo antitumor activity of HER2 tandem CAR-T cells.

(a-b) Schematic representation of the tandem CAR constructs incorporating 4D5 and H2H antigen-binding domains in different configurations (4D5-H2H and H2H-4D5). (c) Flow cytometric analysis of CAR expression in the indicated CAR-T cells. (d) Experimental design of the cytotoxicity assay using EL4-

wtHER2-mCherry target cells and CAR-T cells at various effector-to-target (E:T) ratios, followed by target cell rechallenge. (e-g) Time-course assessment of CAR-T-mediated cytotoxicity at different E:T ratios of 8:1 (e), 4:1 (f), and 2:1 (g). (h) Experimental scheme of in vivo anti-tumor effect analysis. (i) Tumor volumes at day 16 after tumor inoculation in each treatment group: DPBS (control), untransduced $CD8^+$ T cells (UTD), 4D5 CAR-T, H2H CAR-T, 4D5-H2H CAR-T, and H2H-4D5 CAR-T. (j) Survival analysis comparing the therapeutic efficacy of different CAR-T cell treatments. Data are presented as mean ± SEM (e-g, three biological replicates; I-J, n = 5-12 mice per group). Statistical significance was determined by one-way ANOVA with Tukey's multiple comparisons test (i) and by log-rank (Mantel-Cox) test (j) (*P < 0.05, **P < 0.01, ***P < 0.001, ****P < 0.0001).

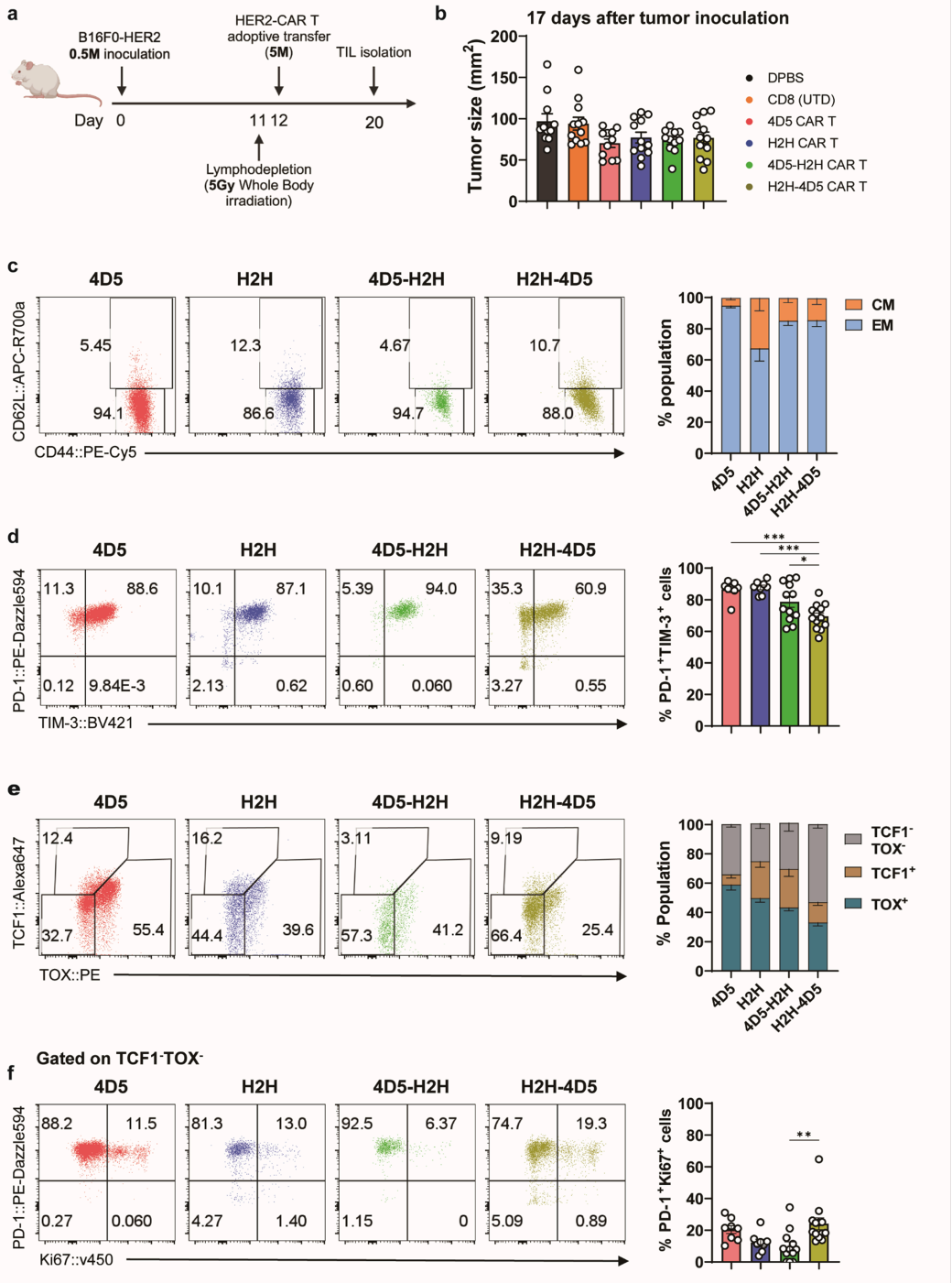


Figure 4

Figure 4

Phenotypic and functional characterization of tumor-infiltrating HER2 tandem CAR-T cells.

(a) Experimental timeline for tumor-infiltrating lymphocyte (TIL) analysis. C57BL/6 mice were inoculated subcutaneously with 5 × 10^5 B16F0-HER2 cells on day 0, received lymphodepletion by 5-Gy whole-body irradiation on day 11, and underwent adoptive transfer of 5 × 10^6 HER2 CAR-T cells on day 12. TILs were

isolated on day 20. (b) Tumor size on day 17 after tumor inoculation in mice receiving DPBS, untransduced $CD8^+$ T cells (UTD), or the indicated HER2 CAR-T cell products. (C–F) Flow cytometric characterization of $CD8^+Thy1.1^+$ CAR TILs expressing the 4D5, H2H, 4D5-H2H, or H2H-4D5 constructs. (c) Representative CD44 and CD62L staining and quantification of central memory (CM; $CD44^+CD62L^+$) and effector memory (EM; $CD44^+CD62L^-$) populations. (d) Representative PD-1 and TIM-3 staining and quantification of $PD\text{-}1^+TIM\text{-}3^+$ cells among CAR TILs. (e) Representative TCF-1 and TOX staining and quantification of the $TCF\text{-}1^-TOX^-$, $TCF\text{-}1^+$, and TOX^+ populations, as defined by the indicated gates. (f) Representative PD-1 and Ki67 staining within the $TCF\text{-}1^-TOX^-$ CAR TIL population and quantification of $PD\text{-}1^+Ki67^+$ cells within this gate. Numbers in flow cytometry plots indicate the percentages of cells within the indicated gates. Data are presented as mean ± SEM. Statistical significance was determined by one-way ANOVA (*P < 0.05, **P < 0.01, ***P < 0.001, ****P < 0.0001).

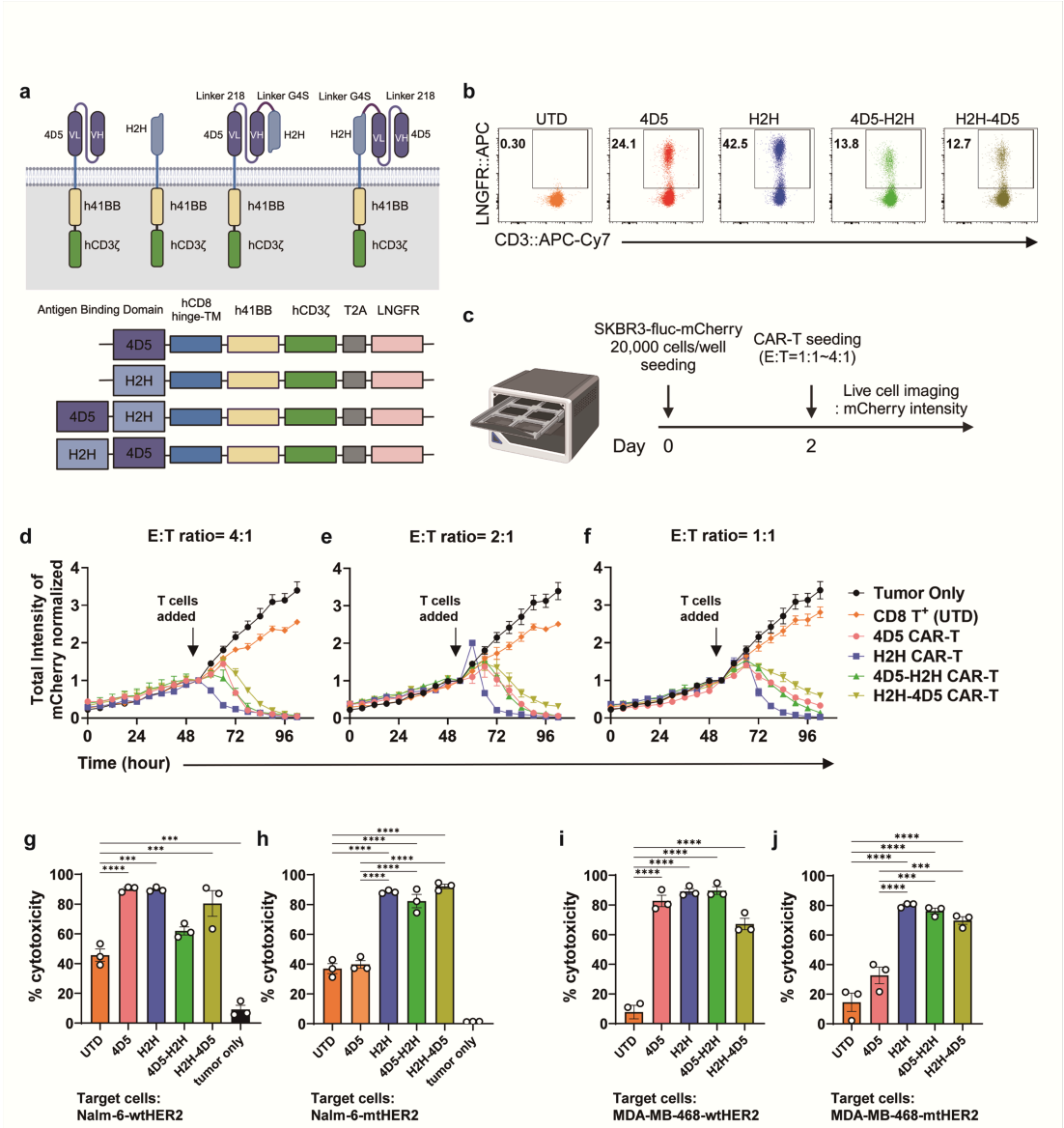


Figure 5

Figure 5

Characterization and cytotoxicity of human HER2-targeting CAR-T cells.

(a) Schematic of the human 4D5, H2H, 4D5-H2H, and H2H-4D5 CAR constructs. (b) Representative flow cytometry plots and quantification of CAR expression in transduced T cells, assessed by LNGFR and CD3 staining. (c) Experimental design of the cytotoxicity assay using SKBR3-fluc-mCherry cells. Tumor cells

were seeded on day 0, and CAR-T cells were added at the indicated effector-to-target (E:T) ratios. mCherry fluorescence intensity was monitored by live-cell imaging. (d-f) Cytotoxicity at E:T ratios of 4:1 (d), 2:1 (e), and 1:1 (f). (g-h) Cytotoxicity against Nalm-6 cells expressing wild-type HER2 (g) or mutant HER2 (h). Target cells were co-cultured with CAR-T cells at an E:T ratio of 1:1. Specific cytotoxicity was measured after 18 h using a flow cytometry-based killing assay. (i-j) Cytotoxicity against MDA-MB-468 cells expressing wild-type HER2 (i) or mutant HER2 (j). GFP-expressing target cells were co-cultured with CAR-T cells at an E:T ratio of 1:1, and total GFP intensity was monitored by CELLCYTE X live-cell imaging. The total GFP intensity in each well was normalized to its value at 12 h, when CAR-T cells were added. Cytotoxicity at 36 h was calculated as [1 − (normalized intensity of the sample / normalized intensity of the tumor-only control)] × 100. Data are presented as mean ± SEM. Statistical significance was determined by one-way ANOVA (*P < 0.05, **P < 0.01, ***P < 0.001, ****P < 0.0001).

Supplementary Files

This is a list of supplementary files associated with this preprint. Click to download.

- Supplefigure2.tif
- Supplefigure1.tif
- 2026H2HManuscriptsupplementalinfomation.docx